MECHANICAL, AND TRIBOLOGICAL PROPERTIES OF TI/TIN BILAYERS: THE DEPENDENCE OF TI INTERLAYER THICKNESS

PROPIEDADES MECÁNICAS, Y TRIBOLÓGICAS DE LA BICAPA TI/TIN: DEPENDENCIA DEL ESPESOR DE LA INTERCAPA DE TI

JHONATTAN DE LA ROCHE YEPES

Ing, Laboratorio de Física del Plasma, Universidad Nacional de Colombia, Manizales-Colombia, jhonattandelaroche@gmail.com

JUAN MANUEL GONZALEZ CARMONA

MsC, RDAI, Universidad del Valle, Cali-Colombia, juanmgonzalezc@gmail.com

ALEXANDER RUDEN MUÑOZ

PhD, Departamento de Matemáticas, Universidad Tecnológica de Pereira, Pereira-Colombia, arudenm@gmail.com

ELISABETH RESTREPO PARRA

PhD, Laboratorio de Física del Plasma, Universidad Nacional de Colombia, Manizales-Colombia, erestrepop@unal.edu.co

FEDERICO SEQUEDA OSORIO

PhD, RDAI, Universidad del Valle, Cali-Colombia, fsequeda@yahoo.com

Received for review November 4th, 2011, accepted February 5th, 2013, final version February, 15 th, 2013

ABSTRACT: Ti/TiN bilayers were grown on AISI 316L stainless steel and Dynasil (SiO_2) substrates, by using a reactive DC magnetron sputtering system. The Ti interlayer was grown at different thicknesses (0, 50, 100, and 200 nm) in order to study their influence on the morphological, mechanical, and tribological properties of the bilayers. The coatings' morphology was determined using an XP2 profilometer adhesion was measured using micro-scratch test equipment, mechanical properties were obtained by a NANOVEA IBIS–Technology nanoindenter with the Oliver-Parr method. Tribological characterization was carried out with a CSEM tribometer, and wear coefficient was obtained by the Archard law by relating the wear area (measured by profilometry). Results present a decrease in the roughness as the interlayer was added. A maximum hardness and elastic modulus of 22 and 310 GPa, respectively, were obtained. On the other hand, the system with an interlayer of 100 nm exhibited the highest adhesion with a critical load of 28 N. Moreover, the system with an interlayer of 200 nm showed an improvement in the tribological behavior due to its great load capability, lower substrate deflection, and low wear rate.

KEYWORDS: interlayer thickness, surface properties, coefficient of friction, wear

RESUMEN: Se depositaron bicapas de Ti / TiN en sustratos de acero inoxidable AISI 316L y Dynasil (SiO_2), mediante el uso de un sistema de magnetrón Sputtering reactivo DC. La intercapa de Ti se creció a diferentes espesores (0, 50, 100, y 200 nm) con el fin de estudiar su influencia en la morfología y en las propiedades mecánicas y tribológicas. La morfología de los recubrimientos se determinó usando un perfilómetro XP2, la adhesión se midió utilizando un equipo de micro scratch-test, las propiedades mecánicas se determinaron mediante un nanoindentador marca NANOVEAIBIS-Technology por el método de Oliver-Parr. La caracterización tribológica se llevó a cabo empleando un tribómetro CSEM y el coeficiente de desgaste se obtuvo por la ley Archard, relacionando el área de desgaste (medida por perfilometría). Los resultados muestran una disminución de la rugosidad con la adición de la intercapa. La máxima dureza y módulo de elasticidad obtenidas fueron de 22 y 310 GPa respectivamente para el sistema con intercapa de 100 nm; además, este sistema exhibió la más alta adhesión con una carga crítica de 28 N. El recubrimiento con una intercapa de 200 nm mostró una mejoría en el comportamiento tribológico debido a su gran capacidad de carga, menor deformación del sustrato y baja tasa de desgaste.

PALABRAS CLAVE: espesor de intercapa, propiedades de superficie, coeficiente de fricción, desgaste

1. INTRODUCTION

Transition metal nitrides are attractive materials for several applications. For instance, titanium nitride (TiN) is used as surface treatment in cutting tools, electronic devices, medical prosthesis, and as a decorative coating due to high hardness, wear resistance, thermal stability, corrosion resistance, biocompatibility, low electric resistance, a low coefficient of friction (COF), and gold-like attractive color [1–5]. One common process in coating production by physical vapor deposition (PVD) consists of including a low-thickness interlayer between the substrate and the

coating, named *seed layer*, *adhesion layer*, or *buffer layer* [3]. This layer is used to improve the adhesion of the final system, in order to minimize the influence of strains generated by a lack of chemical synergy, coupling between crystalline structures, and expansion coefficient differences with substrate used as the base material. As a general statement, the production of an interface between substrate and the film improves the adhesion behavior of the obtained system [6]. In the case of diamond-like carbon (DLC) deposited on steel, the use of silicon, titanium, and their carbides, avoids graphitization, increases chemical affinity, and stabilizes carbon-carbon bonds [7]. In silicon devices, the use of a CuW or Cu (WN) interlayer provides high thermal stability and low electrical resistivity, supplying a metallization barrier [8]. Interlayers of Ti are commonly used, because the element presents a good chemical affinity between substrate superficial oxides and the TiN layer; besides this, the nitride interdiffusion zone is incremented, improving adhesion [3]. From the crystallographic point of view, high texturizing of the Ti layer in (002) crystalline plane promotes preferential orientation of TiN in the (111) crystallographic plane [3,9]. Due to these facts, the use of a Ti interlayer will generate high TiN texturizing, improving properties such as hardness (H), elastic module (E) and plastic deformation resistance (H^3/E^2), which usually indicate improvement in the tribological behavior [9].

TiN and Ti/TiN have been widely studied, and they have been produced by several methods, characterized in a wide range of properties. Nevertheless, in this work, a detailed study of Ti/TiN bilayers, presenting morphological, mechanical, tribological, and corrosive properties is carried out, depending on the Ti interlayer thickness. All of the properties were correlated between them. Special attention was paid to the wear profiles analysis carried out after the ball on disc studies, showing the interlayer effect on the adherence, depending on its thickness. This kind of result is not widely shown in other articles.

In this paper, the effect of Ti interlayer thickness in the superficial, mechanical, tribological, and corrosion-resistance properties of DC magnetron sputtering deposited TiN thin films is studied to obtain the optimum interlayer value and their relationship with coating behavior.

2. EXPERIMENTAL SET-UP

TiN and TiN/$Ti_{(x)}$ (x = 0, 50, 100, and 200 nm of thickness) were deposited on AISI 316L stainless steel and dynasil (this material was used to measure intrinsic stress). Samples were polished and deeply cleaned with an ultrasonic cube in acetone for 15 min in order to eliminate remaining impurities. Thin films were deposited by the reactive magnetron sputtering DC technique, in AJA ATC 1500 equipment [10,11], using Ti (99.9% purity) target of a 5 cm diameter. Base pressure in the reaction chamber was in the order of 10^{-4} Pa. Prior to the deposition, plasma cleaning was carried out during 15 min for removing any impurities and surface oxide layers on the substrate surface. The work pressure was 0.4 Pa and target power density was 5 W/cm^2, and Ar/N_2 gas flow was 10/0.15 sccm. Structural characterization was performed with a Bruker AXS D8 advance X-ray difractometer (XRD), used with a grazing incidence with Cu-k_α radiation (λ = 1.5406 Å) ranging between 30°–80° with steps of 0.02°. The morphological characterization, thickness, roughness, and intrinsic strain using the curvature radiox| and the Stoney equation [12] of the obtained films were determined by an Ambios Technologies XP2 profilometer, using 0.4 mm distance and a range of 10 μm for measuring roughness and 5 mm distance and 100 μm range for obtaining the sample curvature. Adhesion was determined using MICRO TEST scratch test equipment with a diamond Rockwell C 200 μm radius indenter and a 1 N/seg travel speed. Mechanical properties were obtained using a NANOVEA IBIS–Technology nanoindenter with the Oliver-Parr method, a diamond Berkovish indenter, and penetration below 10% of the total coating thickness in order to disregard substrate effects on the obtained measurement [13]. The tribological characterization was performed in a CSEM tribometer using a 6 mm diameter Al_2O_3 counterface ball, 1 N normal applied load, and 10 cm/seg lineal velocity. Wear coefficient was obtained by Archard law, which relates the wear area (measured by profilometry) with the work done on the material [14].

3. RESULTS AND ANALYSIS

3.1 X-ray diffraction

Figure 1 shows the diffraction pattern for TiN with an interlayer of 50 nm. Diffraction peaks corresponding to the crystallographic planes (111), (200), (220), and (311) at 34.2°, 39.8°, 59.1°, and 86.1°, respectively, are observed. These peaks are characteristic of the fcc phase of TiN [17,18]. The fcc structures possess higher mechanical and tribological properties than others such as h.c.p-$Ti_{1-x}N$ [18]. No significant differences in the

system structure were observed since Ti interlayers at different thicknesses were included.

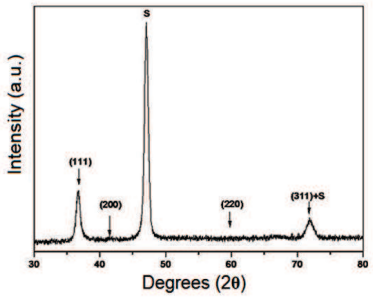

Figure 1. Diffraction pattern of the TiN/Ti_{50nm} bilayer grown by magnetron-sputtering DC

Figure 2 shows the average roughness (R_a) and mean square roughness (R_q) evolution as a function of the Ti interlayer thickness. As was observed, the roughness decreases as an interlayer is deposited. The use of these interlayers was effective in enhancing the nucleation density of coatings [17].

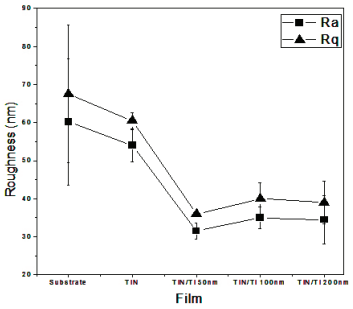

Figure 2. Average roughness (R_a) and mean square roughness (R_q) as a function of the titanium interlayer thickness

The reduction in the film roughness while a Ti interlayer was deposited can be immediately understood as arising from denser and more uniform nucleation, promoting vertical growth versus an initial three-dimensional growth around fewer nucleating seeds [18]. This behavior is in agreement with previous observations of films growth clusters around a low-density of seeds [19]. Differences in the surface roughness may be explained by the difference in their microstructures. This also suggests that the addition of a Ti interlayer reduces the surface roughness of the system; nevertheless, according to the curves tendency, an increase in the thickness of the Ti interlayer does not significantly affect the roughness of the system [20]. A similar case is reported in the literature by Neubauer et al. [21] for copper carbon nanocomposites with an interlayer of Ti. In the latter case, the roughness increases until the film thickness reached 15 nm; after that, there is no observable influence of the Ti-layer thickness on surface topography.

3.2. Adhesion

Figure 3(a) shows Ti interlayer thickness effect in the intrinsic stress and the adhesion (critical load L_c) of the deposited system. The film without interlayer presented higher dispersion caused by an irregular substrate deformation, generated by the film stress. As the interlayer thickness is increased, a decrease in the intrinsic stress was observed because Ti film supports the Ti and N atoms or TiN molecule bombardment, presenting plastic deformation and avoiding perturbations on the TiN lattice [22]. Moreover, the role of the Ti interlayer is to dissolve any oxide layer remaining on the surface of the substrate as well as to relieve shear stress in the interface [3,14,23,24]. Results also show a decrease in the stress up to a certain interlayer thickness value. Nevertheless, after this value, the stress tends to be stable. This indicates that there is a critical Ti interlayer thickness for effectively relieving residual stress [3,9,25].

The scratch test was performed in order to study the film's adhesion. Figure 3 (a) shows an increase on the critical load as the Ti interlayer thickness increases. Due to the TiN film interdiffusion increment, intrinsic stress diminution and total thickness increase, the load capability is enhanced [3]. This behavior avoids film delamination; nevertheless, it has been found that higher-thickness ceramic films can reduce adhesion due to a high dislocation density on the interface [23].

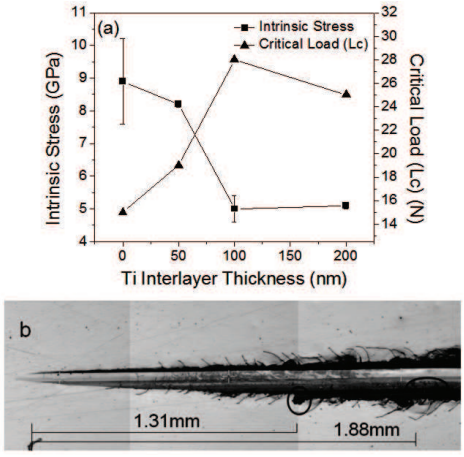

Figure 3. (a) Intrinsic stress and critical load as a function of the interlayer thickness and (b) 10x micrograph of the TiN/$Ti_{100\ nm}$ scratch test

For thicker films, not only the delamination is avoided, but also the spalling degree becomes lower as the load is increased. This demonstrates that the increase of film thickness from a certain critical value can improve film adhesion [26]. As is observed in Fig. 3, the critical thickness for the stress stabilization matches up with the value at which the critical load decreases. The maximum critical load is presented at 100 nm of interlayer thickness. A 10x micrograph (Fig. 3(b)) shows the failure mechanism presented on the TiN/$Ti_{100\ nm}$ sample. It exhibits lateral crack formation on the first millimeters of the track. Partial film delamination (recovery spallation) is observed at 1.31 mm. After 1.88 mm, cracks are observed in the track. This type of failure is called *bulking spallation*, which is presented in the form of irregular arcs on the track. These failures are generally presented in hard films deposited on ductile substrates [27]. Hardness and elastic moduli plots versus penetration depth were obtained by nanoindentation.

3.3. Hardness

Figure 4 shows plots of TiN/$Ti_{200\ nm}$ hardness and elastic modulus as a function of the depth penetration. Maximum values were around 18.5 GPa and 260 GPa, respectively. Figure 4(a) shows a hardness decrease as the penetration depth increases. The vertical line indicates 10% of the total system thickness. The 10% rule refers to the maximum penetration depth to which an indentation test can produce substrate independent hardness measurements. Standard nanoindentation experiments using the Oliver–Pharr scheme [28] have repeatedly shown that the hardness of crystalline materials often shows strong indentation depth dependence, with higher indentation hardness obtained at smaller indentation depths [29,30]. This phenomenon is generally referred as *indentation size effect* (ISE). Nix and Gao [31] explained the ISE measured by using the concept of geometrically necessary dislocations (GND) in which the GND density increases with decreasing indentation depth, resulting in the ISE of hardness for crystalline materials [32]. Often, researchers will forego the limitation and apply the rule as a general limitation for all mechanical properties including Young's modulus [15,33]. The errors present in the measurements probably occur because of asperities [34]. According to figure 4(a), the hardness of the system decreases to the substrate hardness as the depth of penetration increases.

Figure 4(b) shows the behavior of the elastic modulus for the TiN/$Ti_{200\ nm}$ system as a function of the penetration depth that was varied between 0.05 and 1.5 μm. Initially, Young's modulus shows a transition from the TiN modulus (around 280 GPa [35]) to the TiN/Ti composite modulus of around 260 GPa [3], after 1.5 μm of penetration depth. Then, a new transition is observed from a Ti/substrate composite modulus and the subsequent tendency to the stainless steel 316L Young's modulus (160–193 GPa) [36].

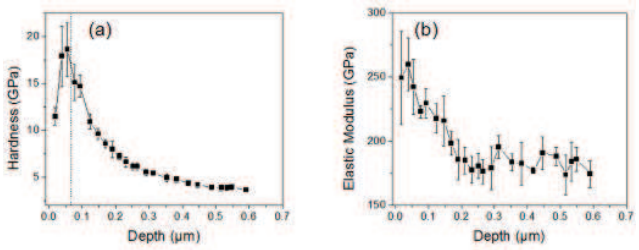

Figure 4. Mechanical properties as a function of indentation depth for TiN/Ti_{200nm} (a) hardness and (b) elastic modulus

In Fig. 5, the hardness and elastic modulus of Ti/TiN coatings depending on the interlayer thickness are observed. Keeping the error bars into account, no tendency was observed. Values were obtained by carrying out a penetration depth lower that 10% of the TiN monolayer thickness (indentation size effect), in order to avoid the substrate and interlayer effect on the system, because the interlayer objective is to improve adherence.

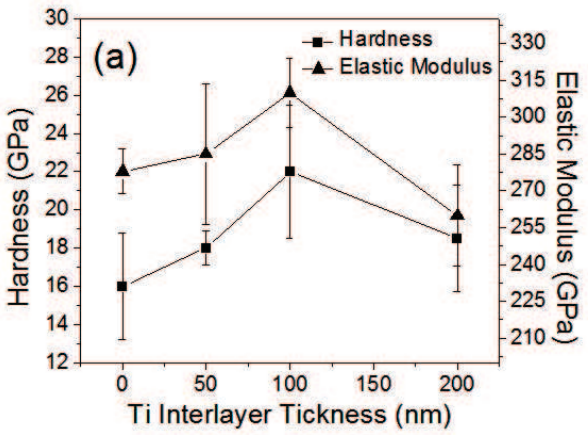

Figure 5. Mechanical properties of the TiN/Tix thin films as a function on the interlayer thickness (a) hardness

3.4. Wear Analysis

Figure 6(a) shows the coefficient of friction (COF) behavior as a function of sliding distance for the substrate and Ti/TiN bilayers, varying the interlayer thickness. Curve *A* shows the COF for the substrate, presenting a strong increase at around 10 m. When the film was deposited on the substrate, the system presents better behavior, increasing the distance of failure. Failures occur when the critical thickness is reached after a certain sliding distance due to ongoing wear [37]. The TiN coating without an interlayer (curve *B*) presented a higher distance of failure but did not show a decrease in the COF. No transitions are observed since it was not possible to determine the COF. This behavior is attributed to high roughness, low adhesion, and delamination due to high intrinsic stress. As the interlayer thickness increases, the distance of failure also increases dramatically. The TiN/Ti_{50nm} presented a COF of 0.6 (with a failure of around 40 m). The TiN/Ti_{100nm} and TiN/Ti_{200nm} showed a COF of approximately 0.2, failing at around 100 m. Again, roughness plays an important role in COF behavior. Tang et al. [38] studied the COF for TiC films grown with and without metallic interlayers of Cr and Ti. They reported that it had less stick-slip and showed more stable friction and wear behavior in films with interlayers than those without any interlayer. The TiN coating without an interlayer was scratched and grooved severely. According to the author, films with a metallic interlayer present cracks which gradually appear on the wear surface. The cracks were caused by the pin or ball sliding repeatedly on the coating surface under applied loads. Nevertheless, in films without an interlayer, islands (particles) appear before the cracks even when the load was increased strongly (when coatings are seriously delaminated). It seems that the coatings without an interlayer are directly torn off because of the poor adhesion between the coating and the substrate [39] while coatings containing a metallic interlayer first underwent a process of wear-track cracking before the delamination happened on the contacting surface. The cracks on a friction surface should be a sign of the islands formed at the later stage of the wear process.

Figure 6 (b) shows the wear coefficient (*k*) of the TiN/Ti_x. As is shown, *k* decreases as the interlayer thickness increases, due to higher adhesion and lower intrinsic stress, because poor adhesion is the predominant wear mechanism.

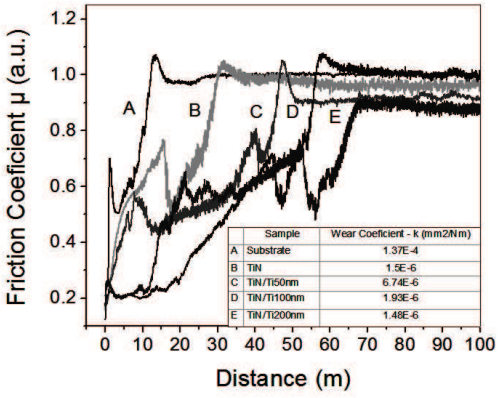

Figure 6. Coefficient of friction as a function of sliding distance by using the ball on disk test for the substrate and TiN/Tix films with different Ti interlayer thickness

Figures 7(a) and (b) show wear profiles for the TiN/Ti_{100nm} and TiN/Ti_{200nm}. Films without interlayer present failure between 20 to 40 meters. On the other hand, a metallic interlayer increases the film's durability. The predominant wear mechanism in all systems is composed of an adhesion-abrasion combination due to hard particle liberation in the wear track, acting as an abrasive mechanism during the test [15]. The TiN/Ti_{100nm} and TiN/Ti_{200nm} failed between 80 to 100 m. Although the TiN/Ti_{100nm} system presents high particle adhesion (a profile higher than the coating surface), the TiN/Ti_{200nm} also presents abrasion. According to the literature, if the metallic interlayer is too thick, there might be high strains due to a plastic deformation of the softer metal which might cause an over critical bending of the ceramic layer, and thus wear increases or a failure of the coating can take place. Holmberg et al. showed that the deformations that are induced during a scratch test on a coated surface result in the bending of the coating [40]. In their investigations, the bond layer strains were higher for a compliant bond layer (like, in our case, Ti) than for a stiff bond layer, but were independent of the thickness. However, a thinner compliant bond layer should be stiffer than a thicker compliant bond layer of the same material. This would imply that a very thick compliant layer might show a considerably higher strain compared to a significantly thinner compliant layer, and thus, induce a higher bending of the hard coating above. It might be assumed that the TiN coating reached the critical thickness after a certain sliding distance due to wear. Thus, it might be argued that there is a Ti/TiN thickness ratio for a

given TiN thickness that yields a significant decrease in wear. This thickness ratio might also depend on the mechanical load and the coating properties, and might be different; e.g., for other coating systems [37].

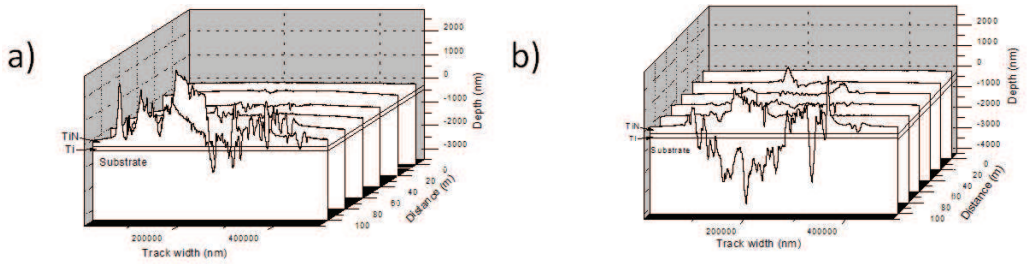

Figure 7. Wear profiles of: (a) TiN, (b) TiN/Ti_{50nm},(c) TiN/Ti_{100nm}, and (d) TiN/Ti_{200nm}

As a final remark, including a Ti interlayer between the TiN coating and the substrate can improve system performance, especially in properties such as adhesion, and friction coefficient. These properties are also affected by the interlayer thickness that normally has a critical value. For example, for the adhesion and the friction coefficient performance, thicker interlayers might generate high strains due to the plastic deformation of the softer metal, causing strong bending of the ceramic layer and producing an increase in wear and failures in the system. On the other hand, the hardness is more affected by the indentation depth and its relationship with system thickness.

4. CONCLUSIONS

The Ti interlayer thickness influence on TiN/Ti coatings behavior produced by the reactive magnetron-sputtering DC technique was studied. The improvement of most of the system properties was observed with the inclusion of the Ti interlayer. Hardness and Young's modulus were more influenced by the indentation depth than the interlayer thickness. On the other hand, roughness, adherence, wear, and corrosion resistance were improved by including the metallic interlayer. Nevertheless, for properties such as adherence and wear resistance, a very thick interlayer can present a considerably higher strain, inducing a higher bending of the hard coatings.

ACKNOWLEDGMENTS

The authors gratefully acknowledge the financial support of the *Instituto Colombiano para el Desarrollo de la Ciencia y la Tecnología* (COLCIENCIAS) during the course of this research, under project of doctoral fellowships, 2005. The authors also acknowledge the *Escuela de Ingeniería de Materiales* of the *Universidad del Valle* and the *Laboratorio de Física del Plasma* of the *Universidad Nacional de Colombia, Sede Manizales*.

REFERENCES

[1] Ono, T., Uemura, M. and Yatsuzuka, M., Adhesion improvement of TiN film on tool steel by a hybrid process of unbalanced magnetron sputtering and plasma-based ion Implantation, Phys. Res. B, 257,pp. 786-789, 2007.

[2] Restrepo, E., Arango, P. J. and Casanova, S., Algunos conceptos sobre nitruro de titanio y el carburo de titanio, Dyna, 76, pp. 213-224, 2009.

[3] Huang, J.H., Ouyang, F.Y. and Yu, G.P., Effect of film thickness and Ti interlayer on the structure and properties of nanocrystalline TiN thin films on AISI D2 steel Surface & Coatings Technology, 201, pp. 7043–7053, 2007.

[4] Devia, A., Restrepo, E., Segura, B., Arango, Y. C. and Arias, D. F., Study of TiN and Ti/TiN coatings produced by pulsed-arc discharge, Surface & Coatings Technology, 190, pp. 83-89, 2005.

[5] Kim, G.S., Lee, S.Y., Hahn, J.H., Lee, Y., Hand, J.G., Lee, J.H. and Lee, S.Y., Effects of the thickness of Ti buffer layer on the mechanical properties of TiN coatings, Surface & Coatings Technology, 171, pp. 83-90, 2003.

[6] Gerth, J. and Wiklund, U., The influence of metallic interlayers on the adhesion of PVD TiN coatings on high-speed steel, Wear, 264, pp. 885-892, 2008.

[7] Kwang-Ryeol, L., Kwang Yong, E., Inyoung, K. and Jongryoul, K., Design of W buffer layer for adhesion improvement of DLC films on tool steels, Thin Solid Films, 377-378, pp. 261-268, 2000.

[8] Chu, J.P., Lin, C.H. and John, V.S., Barrier-free Cu metallization with a novel copper seed layer containing various insoluble substances, Vacuum, 83, pp. 668-671, 2009.

[9] Huang, J.H., Ma, C.H. and Haydn, C., Effect of Ti interlayer on the residual stress and texture development of TiN thin films, Surface & Coatings Technology, 200, pp. 5937–5945, 2006.

[10] Murcia, A., Ruden, A., Neira, A., Gonzalez, J.M., Castro, I., Brulh, S. and Sequeda, F., Tribological Properties of Duplex Coating Applied in Chrome Based Steel, Society Vacuum Coaters , 505, pp. 856-860, 2009.

[11] Ruden, A., Restrepo, J. S., Muñoz, M., Gonzalez, J. M., Neria, A. and Sequeda, F., Efecto del flujo de nitrógeno en la estructura, orientación preferencial y análisis DFT de ZrN depositado por pulverización Magnetrónica reactiva, Suplem. Revista Latinoamericana de Metalalurgia y Materiales, S1, pp. 1009-1013, 2009.

[12] Ohring, M., Materials science of thin films, Academic press, New York, 2002.

[13] Fischer-Cripps, A.C., Handbook of Nanoindentation, Fischer-Cripps Laboratories Pty Ltd, Forestville, Australia, 2009.

[14] Bates, T. R., Ludema, K. C. and Brainard, W. A., A rheological mechanism of penetrative wear, Wear, 30, pp. 365-375, 1974.

[15] Devia, D. M., Restrepo, J., Ruden, A., González, J.M., Sequeda, F. and Arango. P.J., Society Vacuum Coaters, 505 pp. 32-36, 2009.

[16] Kasukabe, Y., Nishida, S., Yamamoto, S., Yoshikawa, M. and Fujino, Y., Atomistic nitriding processes of titanium thin films due to nitrogen-implantation, Applied Surface Science, 254, pp. 7942-7946, 2008.

[17] Fu, Y., Yan, B. and Loh, N. L., Effects of pre-treatments and interlayers on the nucleation and growth of diamond coatings on titanium substrates, Surface and Coatings Technolgy, 130, pp. 173-185, 2000.

[18] Naguib, N. N., Elam, J. W., Birrell, J., Wang, J., Grierson, D. S., Kabius, B., Hiller, J. M., Sumant, A. V., Carpick, R. W., Auciello, O. and Carlisle, J. A., Enhanced nucleation, smoothness and conformality of ultrananocrystalline diamond (UNCD) ultrathin films via tungsten interlayers, Chemical Physics Letters, 430, pp. 345-350, 2006.

[19] Sumant, A. V., Grierson, D. S., Gerbi, J. E., Birrell, J., Lanke, U. D., Auciello, O., Carlisle, J. A. and Carpick, R. W., Toward the Ultimate Tribological Interface: Surface Chemistry and Nanotribology of Ultrananocrystalline Diamond, Advanced Materials, 17, pp. 1039-1045, 2005.

[20]. Wo, P.C., Munroe, P.R., Zhou, Z.F., Li, K.Y. and Xie, Z.H., Effects of TiN sublayers on the response of TiSiN nanocomposite coatings to nanoidentation and scratching contacts, Materials Science Engineering A, 527, pp. 4447-4457, 2010.

[21] Neubauer, E., Eisenmenger-Sittner, C., Bangert, H. and Korb, G., AFM and AUGER investigations of as-deposited and heat treated copper coatings on glassy carbon surfaces with titanium intermediate layers, Vacuum, 71, pp. 293-298, 2003.

[22] Pierson, H. O., Handbook of Refractory Carbides and Nitrides: Properties, Characteristics, Processing and Applications, Noyes Publications, New Jersey, 1996.

[23] Leoni, M., Scardi, P., Rossi, S., Fedrizzi, L. and Massiani, Y., (Ti,Cr)N and Ti/TiN PVD coatings on 304 stainless steel substrates: Texture and residual stress, Thin Solid Films, 345, pp. 263-269,1999.

[24] Rickerby, D.S., Jones, A.M. and Bellamy, B.A., X-ray diffraction studies of physically vapour-deposited coatings, Surface and Coatings Technology, 37, pp. 111-137, 1989.

[25] Huang, J.-H., Ma, C.H. and Chen, H., Effect of Ti interlayer on the residual stress and texture development of TiN thin films deposited by unbalanced magnetron sputtering, Surface and Coatings Technology, 201, pp. 3199-3204, 2006.

[26] Wei, C. and Yen, J.-Y., Effect of film thickness and interlayer on the adhesion strength of diamond like carbon films on different substrates, Diamond Related Materials, 16, pp. 1325-1330, 2007.

[27] Cordill, M.J., Moody, N.R. and Bahr, D.F., The effects of plasticity on adhesion of hard films on ductile interlayers, Acta Materialia, 53, pp. 2555-2562, 2005.

[28] Oliver, W.C. and Pharr, G.M., An improvement technique for determining hardness and elastic modulus using load displacement indentation experiments ,Journal of Material Research, 7, pp. 1564-1583, 1992.

[29] Manika, I. and J. Maniks., Size effects in micro- and nanoscale indentation**,** Acta Materialia, 54, pp. 2049-2056, 2006.

[30] Feng, G. and Nix, W.D., Indentation size effect in MgO, Scripta Materialia, 51, pp. 599-603, 2004.

[31] Nix, W.D., Gao, H. and Mech, J., Indentation size effects in crystalline materials: A law for strain gradient plasticity, Physics Solids, 46, pp. 411-425, 1998.

[32] Huang, Y., Shen, J., Sun, Y. and Sun, J., Indentation size effect of hardness of metallic glasses**,** Materials Design, 31, pp. 1563-1566, 2010.

[33] Fischer-Cripps, A.C., Introduction to Contact Mechanics, 2nd ed. Springer Science, New York, 2007.

[34] De Souza, G.B., Foerster, C.E., Da Silva, S.L.R., Serbena, F.C., Lepienski, C.M. and Dos Santos, C.A., Hardness and elastic modulus of ion-nitrided titanium obtained by nanoindentation, Surface and Coatings Technology, 191, pp. 76-82, 2005.

[35] Karimi, A., Shojaei, O.R., Kruml, T. and Martin, J.L., Characterization of TiN thin films using the bulge test and the nanoindentation technique, Thin Solid Films, 308–309, pp. 334-339, 1997.

[36] Kluba, A., Bociaga, D. and Dusdek, M., Hydrogenated amorphous carbon films deposited on 316L stainless steel, Diamond Related Materials, 19, pp. 533-536, 2010.

[37] Fontalvo, G. A., Daniel, R. and Mitterer, C., Interlayer thickness influence on the tribological response of bi-layer coatings, Tribology International, 43, pp. 108-112, 2010.

[38] Tang, J., Feng, L. and Zabinski, J. S., The effects of metal interlayer insertion on the friction, wear and adhesion of TiC coatings, Surface and Coatings Technology, 99, pp. 242-247, 1998.

[39] Tang, J., Zabinski, J.S. and Bultman, J.E., TiC coatings prepared by pulsed laser deposition and magnetron sputtering, Surface and Coatings Technology, 9I, pp. 69-73, 1997.

[40] Holmberg, K., Laukkanen, A., Ronkainen, H. and Wallin, K., Surface stresses in coated steel surfaces—influence of a bond layer on surface fracture, Tribology International, 42, pp. 137-148, 2009.